Microbial Cell Factories

RESEARCH Open Access

Integrative analysis of transcriptome and metabolome profiling uncovers underlying mechanisms of the enhancement of the synthesis of biofilm in *Sporobolomyces pararoseus* NGR under acidic conditions

Dandan Wang[1], Nan Zeng[1], Chunji Li[3,4,5], Chunwang Li[2], Yunjiao Wang[2], Bin Chen[2], Jiajia Long[2], Ning Zhang[2*] and Bingxue Li[1*]

Abstract

Background *Sporobolomyces pararoseus* is a well-studied oleaginous red yeast that can synthesize a variety of high value-added bioactive compounds. Biofilm is one of the important biological barriers for microbial cells to resist environmental stresses and maintain stable fermentation process. Here, the effect of acidic conditions on the biosynthesis of biofilms in *S. pararoseus* NGR was investigated through the combination of morphology, biochemistry, and multi-omics approaches.

Results The results showed that the acidic environment was the key factor to trigger the biofilm formation of *S. pararoseus* NGR. When *S. pararoseus* NGR was cultured under pH 4.7, the colony morphology was wrinkled, the cells were wrapped by a large amount of extracellular matrix, and the hydrophobicity and anti-oxidative stress ability were significantly improved, and the yield of intracellular carotenoids was significantly increased. Transcriptome and metabolome profiling indicated that carbohydrate metabolism, amino acid metabolism, lipid metabolism, and nucleic acid metabolism in *S. pararoseus* NGR cells were significantly enriched in biofilm cells under pH 4.7 culture conditions, including 56 differentially expressed genes and 341 differential metabolites.

Conclusions These differential genes and metabolites may play an important role in the formation of biofilms by *S. pararoseus* NGR in response to acidic stress. The results will provide strategies for the development and utilization of beneficial microbial biofilms, and provide theoretical support for the industrial fermentation production of microorganisms to improve their resistance and maintain stable growth.

Keywords *Sporobolomyces pararoseus*, Biofilm, Acid environment, Transcriptomics, Metabolomics

*Correspondence:
Ning Zhang
zhangning@syau.edu.cn
Bingxue Li
libingxue@syau.edu.cn

Full list of author information is available at the end of the article

Introduction

Sporobolomyces pararoseus is a species of red yeast [1, 2], a beneficial yeast that can produce a variety of bioproducts such as microbial oils, surfactants, enzymes, and carotenoids [3–6], and has been widely used in the medical industry, pharmaceuticals, food and health care [5, 6]. However, during industrial microbial fermentation, the growth of yeast cells is subjected to a variety of environmental stresses, in particular, a decrease in ambient pH can increase intracellular reactive oxygen species (ROS) levels, leading to cellular damage, which in turn affects microbial growth and development, and in severe cases, leads to cell death [7], resulting in a significant reduction in the efficiency of metabolite biosynthesis. To date, microorganisms have evolved many resilient ways to sense environmental changes in response to environmental stress [8], such as through cell differentiation [9], spore production [10] and biofilm formation [11, 12]. Among them, biofilm has been widely recognized as a unique growth mode chosen by microorganisms in their natural environment in response to various environmental stresses [13].

Biofilm is a three-dimensional structural material composed of microbial cells and extracellular polymeric substances (EPS) [14, 15], which is commonly manifested by the formation of wrinkled colonies [16], and has the properties of increased adhesion, decreased motility, increased hydrophobicity and increased resistance to hydrogen peroxide [17, 18]. Therefore, biofilm can be used as a ' protective suit ' for microorganisms to help them resist various environmental stresses, including nutritional deficiencies, extreme temperatures, acid, alkaline environments, ultraviolet rays, and disinfectants [19–23]. Research on microbial biofilm has primarily focused on bacterial systems, leading to substantial advancements in understanding their taxonomy, development, structural organization, and functional roles [21, 24]. Fungal systems, in contrast, have been studied to a smaller degree, with *Candida albicans* and *Saccharomyces cerevisiae* being the most extensively researched species. These studies have primarily concentrated on clinical infections and strategies to inhibit biofilm formation [19, 24]. In comparison, research on *Sporobolomyces pararoseus*, a beneficial microorganism known for its pigment production, remains limited. Investigations into the environmental factors influencing biofilm formation and the role of this microorganism in stress resistance are sparse [1, 2]. Therefore, it is significance to increase the in-depth study and exploitation of biofilms of beneficial fungi for their application in the fields of pharmaceutical industry, food industry, agricultural production, environmental protection, energy utilization, and industrial fermentation production.

The prime purpose of this study was to investigate the effect of acidic conditions on the biofilm formation in *S. pararoseus* NGR. At the same time, the macroscopic three-dimensional structure of biofilm was observed by scanning electron microscope and its hydrophobicity was measured. In addition, the polysaccharide, protein, eDNA content and oxidative stress ability of biofilm extracellular EPS were evaluated, and the intracellular carotenoid synthesis level was explored. Moreover, transcriptome and metabolome sequencing techniques were used to study the differences in gene expression profiles and metabolites of *S. pararoseus* NGR under acid stress, aiming to analyze the differences between wrinkled biofilm colonies and non-biofilm colonies of *S. pararoseus* NGR. The detailed study of biofilm formation in *S. pararoseus* NGR provides insights into the mechanisms of abiotic stress, supports normal growth, enhances metabolite biosynthesis, and offers a valuable reference for investigating the mechanisms underlying biofilm formation and the development of colony morphology.

Materials and methods

Yeast strain and culture conditions

The *S. pararoseus* NGR (CGMCC 2.5280) used in this study was derived from the surface of strawberry fruit. *S. pararoseus* NGR was inoculated in liquid medium containing 100 mL YPD (glucose: 10 g/L; peptone: 10 g/L; yeast extract powder: 5 g/L; pH 6.0) in a conical flask at 28 °C, 180 rpm for 24 h as the pre-seeding solution. Subsequently, the pre-seed liquid was transferred to a new conical flask containing 100 mL YPD medium according to the inoculation amount of (1%, v/v) and cultured at 28 °C, 180 rpm for 24 h as the seed liquid.

Effects of different pH conditions on the colony morphology and growth of *S. pararoseus* NGR

The seed solution was inoculated with 10 μL of YPD solid and liquid media at pH 3.0, pH 4.0, pH 4.7, pH 5.0, pH 6.0 (control), pH 7.0 and pH 8.0, respectively, and their colony phenotypes were observed. Subsequently, the seed solution was inoculated into a 96-well polystyrene microtitration plate at a (1%, v/v) inoculation amount, with 6 replicates per treatment, and cultured at 28 °C, 180 rpm for 96 h. The optical density value at cell growth level was measured at 560 nm by using a BioTek Cytation5 microplate reader (DERICA BIOTECH, Beijing Delika Biotechnology Co., Ltd., Beijing, China).

Determination and analysis of biofilm

The liquid medium with pH 3.0, pH 4.0, pH 4.7, pH 5.0, pH 6.0 (control), pH 7.0, pH 8.0 was placed in a 96-well polystyrene microtitration plate (200 μL per well), and then the seed liquid was inoculated into a 96-well polystyrene microtitration plate according to the inoculation

amount of (1%, v/v). Each treatment had 6 replicates. The cells were cultured at 28 °C for 24 h. After culture, the medium was removed and washed with 0.1 M phosphate buffer (pH 7.2) to remove planktonic cells.

The biofilm yield of *S. pararoseus* NGR under different pH conditions was quantified using crystal violet (CV) staining [25], 200 μL of methanol was added to each well for 15 min of fixation, and 200 μL of CV (1%, v/v) was added to each well for 5 min of staining after natural air-drying of the methanol was aspirated. Subsequently, excess dye was removed by washing with sterile water. Finally, 200 μL of glacial acetic acid (33%, v/v) was added to each well and placed at 32 °C for 30 min. The optical density was measured at 590 nm by using the Bio Tek Cytation5 microplate reader (DERICA BIOTECH, Beijing Delika Biotechnology Co., Ltd., Beijing, China).

Biofilm morphology analysis of *S. pararoseus* NGR

Scanning electron microscopy was used to observe the colony structure of *S. pararoseus* NGR cultured at pH 6.0 and pH 4.7 for 48 h. The colony size was cut from the agar plate with a knife to 5 * 5 mm, fixed with glutaraldehyde (2.5%, v/v) at low temperature (5–6 °C) for 24 h, and rinsed with 0.1 M phosphate buffer (pH 7.2) for 3 times, 15 min each time. The samples were dehydrated with ethanol (50%, 60%, 70%, 80%, 90%, v/v) for 15 min and anhydrous ethanol for 10 min, respectively, and repeated three times. It was then replaced with tert-butanol (50%, 75%, 90%, v/v) for 10 min, and tert-butanol (100%, v/v) for 10 min and repeated three times. Subsequently, gold (20 nm) was plated with a sputtering coater (MC1000), and the samples were detected by a scanning electron microscope (HITACHI Regulus 8000).

Biofilm hydrophobicity determination

The strength of the relative hydrophobicity of a biofilm surface shows a positive correlation with its degree of stabilization [26, 27]. Cell surface hydrophobicity (CSH) of yeast cells was determined using the microbial adhesion to hydrocarbons (MATH) method [28]. *S. pararoseus* NGR was cultured in YPD solid and liquid media at pH 6.0 and pH 4.7 for 48 h, respectively. After culture, the cells were centrifuged at 12,000 g for 3 min using an Eppendorf 5430R centrifuge (Eppendorf himac Technologies, Hamburg, Germany) and washed twice with phosphate buffer. The *S. pararoseus* NGR cells were then resuspended in 6 mL of 4 M ammonium sulfate PBS to increase the hydrophilicity of the aqueous phase, and 200 μL was taken in a 96-well plate with a Bio Tek Cytation5 zymograph at 650 nm absorbance for (A0). Subsequently, 0.6 mL of xylene was added to the assay tube containing 3 mL of yeast suspension, the tube without xylene was used as a control, the tube was vortexed for 1 min and left at room temperature for 15 min, then 200 μL of the lower aqueous phase was taken in a 96-well plate, and the absorbance of the samples was measured at 650 nm using a Bio Tek Cytation5 enzyme marker (A).

The CSH is calculated as:

$$\mathrm{CSH}\,(\%) = (1 - \mathrm{A}/\mathrm{A0}) \times 100\%$$

Extraction of extracellular polymeric substances (EPS)

Extracellular polymeric substances (EPS) in *S. pararoseus* NGR biofilm were extracted by sodium hydroxide extraction method [29]. Cells were collected after *S. pararoseus* NGR was cultured in YPD solid and liquid medium for 48 h at pH 6.0 and pH 4.7, respectively, and mixed with 20 mL of NaCl solution (0.90%, w/v) in 50 mL centrifuge tubes, centrifuged at 4 °C, 12,000 g for 10 min using an Eppendorf 5430R centrifuge (Eppendorf himac Technologies, Hamburg, Germany), and the supernatant was passed through a 0.45 μm filter membrane to obtain the first filtrate (S-EPS). Then, the precipitated *S. pararoseus* NGR cells were diluted to 20 mL with sodium chloride solution (0.90%, w/v), and the second centrifugation was performed. The EPS was centrifuged at 4 °C 12,000 g for 10 min, and the supernatant was filtered through a 0.45 μm membrane to obtain the second filtrate (LB-EPS). The total EPS in the filtrate determination system of the two supernatants was summarized. The samples were stored in a refrigerator at 4 °C, and then EPS determination and analysis (total polysaccharides, total proteins, and total extracellular DNA) were performed [30, 31].

Determination of total polysaccharide, total protein and extracellular DNA content

200 μL of EPS solution was taken and added to 1.8 mL of water and then mixed with 5.0 mL of phenol (6%, v/v). The mixed solution was heated in a water bath at 96 °C for 20 min and then cooled to room temperature, and the polysaccharide concentration in the EPS solution was determined using a Bio Tek Cytation5 enzyme marker (DERICA BIOTECH, Beijing Delika Biotechnology Co., Ltd., Beijing, China) [32]. Glucose was added to prepare polysaccharide standard solutions (0.02, 0.04, 0.06, 0.06, 0.08, 0.10, 0.12 mg/mL) for calibration.

The protein content of EPS was determined using a BCA (bicinchoninic acid) protein assay kit (Nanjing Jianjian Biotechnology Co., Ltd., Nanjing, China) [31].

The abundance of DNA was determined using diphenylamine colorimetry [33], and its absorbance value was measured at 595 nm using a Bio Tek Cytation5 enzyme marker (DERICA BIOTECH, Beijing Delika Biotechnology Co., Ltd., Beijing, China).

Measurement of intracellular reactive oxygen species (ROS)

The intracellular ROS levels in yeast cells cultured under different pH conditions were determined by using a ROS level kit (Beijing Solarbio Biotechnology Co., Ltd., Beijing, China). The oxidative sensitive probe 2′,7′-dichlorodihydrofluorescein diacetate (DCFH-DA) was used to determine the relative level of ROS in cells under two colony morphologies. The fluorescence intensity was detected by Bio Tek Cytation5 microplate reader (DERICA BIOTECH, Beijing Delika Biotechnology Co., Ltd., Beijing, China). The emission wavelength was set at 525 nm and the excitation wavelength was 488 nm.

Determination of intracellular superoxide dismutase (SOD), catalase (CAT) and total antioxidant capacity (T-AOC)

Yeast cells were collected and placed in a 2 mL centrifuge tube, 9 times the volume of phosphate buffer solution (PBS, pH 7.2) was added, and then the tissue was homogenized by ultrasound under ice water bath conditions. After centrifugation at 12,000 g for 10 min using an Eppendorf 5430R centrifuge (Eppendorf himac Technologies, Hamburg, Germany), the supernatant was transferred to a new EP tube. The relative activity of superoxide dismutase (SOD) was determined by superoxide dismutase analysis kit (Beijing Solarbio Biotechnology Co., Ltd., Beijing, China). Ammonium molybdate colorimetric method was used to determine the relative activity of catalase (CAT) by catalase detection kit (Beijing Box Biotechnology Co., Ltd., Beijing, China). The total antioxidant capacity (T-AOC) was measured using the total antioxidant capacity kit (Beijing Solarbio Biotechnology Co., Ltd., Beijing, China). Bio Tek Cytation5 microplate reader (DERICA BIOTECH, Beijing Delika Biotechnology Co., Ltd., Beijing, China) was used to evaluate intracellular SOD, CAT activity and T-AOC, and the optical density values were set to 450, 405 and 593 nm, respectively.

Extraction and determination of carotenoids

The *S. pararoseus* NGR was cultured in darkness for 96 h in both liquid and solid media at pH 4.7 and 6.0, respectively, to prevent pigment degradation. Every 24 h, the yeast cells were collected by centrifugation at 10,000 g for 10 min at 4 ℃ using an Eppendorf 5430R centrifuge (Eppendorf himac Technologies, Hamburg, Germany), washed twice with sterile water, and freeze-dried for 48 h. An aliquot of 0.1 g of the cells was weighed and subjected to cell wall disruption by adding 2 mL of dimethyl sulfoxide (DMSO), followed by incubation in a water bath at 65 °C for 30 min with intermittent shaking. Subsequently, 6 mL of acetone was added, and the mixture was further incubated in a water bath at 65 °C for 20 min with gentle agitation. The supernatant was then collected by centrifugation at 10,000 g for 10 min. Following the steps outlined above, the carotenoid-containing supernatant was transferred to a new test tube, and the extraction process was repeated until the yeast cells turned colorless. To determine the carotenoid content, an equal volume of n-hexane was added to the collected supernatant and extracted for 10 min. The absorbance of the n-hexane layer was measured using a Bio Tek Cytation5 microplate reader (DERICA BIOTECH, Beijing, China) at a wavelength of 450 nm.

The carotenoid content (μg/g) is calculated using the formula:

$$\text{Content of carotenoid} = (\mathrm{A} \times \mathrm{D} \times \mathrm{V})/(0.16 \times \mathrm{W})$$

where:

A represents the optical density value;

D denotes the dilution factor of the sample during measurement;

V is the total volume of solvent used for extraction;

W signifies the weight of the original bacterial powder;

And 0.16 is the extinction coefficient specific for carotenoids.

Total RNA extraction and transcriptome analysis

S. Pararoseus NGR cells cultured on YPD solid medium at pH 4.7 and 6.0 for 48 h were collected respectively. Total RNA was extracted using TRIzol® Reagent (Takara, Dalian, China), and genomic DNA was removed using DNase I (Takara, Dalian, China). RNA quality was then determined using a 2100 Bioanal (Agilent) Bioanalyzer and quantified using an ND-2000 (Thermo Fisher Scientific, Waltham, MA, USA). High-quality RNA samples (OD260/280=1.8–2.2, OD260/230≥2.0, RIN≥6.5, 28 S:18 S≥1.0, > 10 μg) were used to construct sequencing libraries. Transcriptome sequencing analysis of the samples for comparison was conducted on the Next-Generation Sequencing (NGS) Illumina HiSeq platform. In order to identify differentially expressed genes (DEGs) between cells in two different colony morphologies, the expression level of each gene was calculated using the FRKM method. Differential expression analysis was performed using the R statistical package edgeR (Empirical analysis of Digital Gene Expression in R). DEGs between the two samples were screened using the criteria of logarithm of |log2FC| ≥ 1 and false discovery rate (FDR)≤0.05. The expression levels of the two samples were analyzed by Goatools (https://github.com/tanghaibao/Goatools) and KOBAS (http://kobas.cbi.pku.edu.cn/), and the expression level of each gene was calculated by FRKM method. home.do) for GO functional enrichment and KEGG pathway analysis of differential genes. Differential genes were significantly enriched in GO

and metabolic pathways when the bonferroni-corrected *p*-value of the differential gene was ≤0.05.

Metabolite extraction and metabolome analysis

S. Pararoseus NGR cells cultured on YPD solid medium at pH 4.7 and 6.0 for 48 h were collected respectively. The collected yeast cells (100 mg) were grind separately in liquid nitrogen, homogenized, and resuspended in pre-cooled methanol (80%, v/v) and formic acid (0.1%, v/v). The samples were incubated on ice for 5 min, then centrifuged at 12,000 g, 4 °C for 5 min, and the supernatant was diluted with LC-MS grade water to a final concentration containing methanol (53%, v/v). The samples were then transferred to new Eppendorf tubes and centrifuged at 12,000 g for 10 min at 4 °C.

Subsequently, the supernatants were injected into an LC-MS/MS system for analysis. Untargeted metabolomics analysis was performed using a Vanquish UHPLC system (Thermo Fisher) coupled with an Orbitrap Q ExactiveTM HF-X mass spectrometer (Thermo Fisher). Samples were injected into an Hyperil Gold column (100×2.1 mm, 1.9 μm) using a 16 min linear gradient at a flow rate of 0.2 mL/min. The eluents for the positive polarity mode were eluent A (0.1%, v/v formic acid in water) and eluent B (methanol). The eluents for the negative polarity mode were eluent A (5 mM ammonium acetate, pH 9.0) and eluent B (methanol). The solvent gradient was set as follows: (98%, v/v) A, (2%, v/v) B, 1.5 min; (15%, v/v) A, (85%, v/v) B, 3.0 min; (0%, v/v) A, (100%, v/v) B, 10.0 min; (98%, v/v) A, (2%, v/v) B, 10.0 min; (98%, v/v) A, (2%, v/v) B, 11.0 min; (98%, v/v) A, (2%, v/v) B, 12.0 min. Q Exactive HF-X mass spectrometer was operated in positive/negative polarity mode with spray voltage of 3.5 kV, capillary temperature of 320 ℃, sheath gas flow rate of 35 pis, aux gas flow rate of 10 L/min, s-lens RF level of 60 and aux gas heater temp of 350 ℃. The raw data files generated by UHPLC-MS/MS were processed using the Compound Discoverer 3.0 (CD 3.1, Thermo Fisher) to perform peak alignment, peak picking, and quantitation for each metabolite. After that, peak intensities were normalized to the total spectral intensity. The normalized data were used to predict the molecular formula based on additive ions, molecular ion peaks, and fragment ions. Identification of metabolites in the metabolome was based on databases including HMDB (http://www.hmdb.ca), Metlin (http://metlin.scripps.edu), MassBank (http://www.massbank.jp), LipidMaps (http://www.lipidmaps.org) and mzCloud (https://www.mzcloud.org). Differentially accumulated metabolites (DAMs) were evaluated using partial least squares-discriminant analysis (PLS-DA) and orthogonal partial least squares-discriminant analysis (OPLS-DA) models, with consideration of variable importance in prediction (VIP) scores. The thresholds for the analytical models were set at |log2FC| ≥ 1, OPLS-DA_VIP≥1 and *P*-value≤0.05. Integration of metabolomics and transcriptomics data was performed using Pearson correlation coefficients.

Real-time fluorescent quantitative PCR assay

SYBR Green Premix Pro Taq HS qPCR Kit (AG11718, ACCURATE BIOTECHNOLOGY, HUNAN, Co., Ltd, Changsha, China) was used for qPCR in Quant Studio6 Flex system (Thermo Fisher Scientific, USA). The 26 S rDNA was selected as the internal reference gene, and the relative expression of each gene was calculated by the comparative crossover (CP) method and expressed by the $2^{-\Delta\Delta CT}$ method. Each gene expression analysis was performed using three independent biological repeats. The qPCR specific primers used are shown in Table S1.

Statistical analysis

All experiments were performed in triplicate and data were averaged and expressed as mean±standard error (SE). IBM SPSS 25.0 (SPSS Inc., Chicago, IL, USA) software was used for statistical analysis. Comparison of means across treatments was performed by one-way analysis of variance (ANOVA) with a *P*-value<0.05 and Turkey's significant difference test.

Results

Determination and analysis of colony phenotypes, growth curves and biofilm formation capacity of *S. pararoseus* NGR under different pH conditions

In this study, the colony growth phenotypes of *S. pararoseus* NGR under different environmental pH were investigated to determine the key factors causing changes in colony morphology. The colony morphology in these environments was observed (Fig. 1-A) and the growth rate was determined (Fig. 1-B) at 24, 48, 72 and 96 h, respectively. The results showed that the alkaline environment at pH 7.0 and pH 8.0 showed smooth colonies, and the stronger the alkaline, the smoother the colonies were; when the environmental pH changed to acidic, the colonies appeared to be wrinkled, and the wrinkle formation was more prominent at pH 4.7. It is important to note that the coagulation properties of agar in solid media are adversely affected by decreasing pH levels. Our experimental findings revealed a significant decline in agar solidification when the pH dropped below 4.7, which severely hindered the observation and analysis of subsequent experiments. Consequently, we selected a pH 4.7 as the optimal condition for cultivating *S. pararoseus* NGR biofilms in subsequent experiments. This choice facilitates enhanced observation of colony characteristics and precise quantification of biofilm formation.

Subsequently, the effects of different pH conditions on the growth of *S. pararoseus* NGR were analyzed. The results showed that alkaline (pH 8.0) conditions

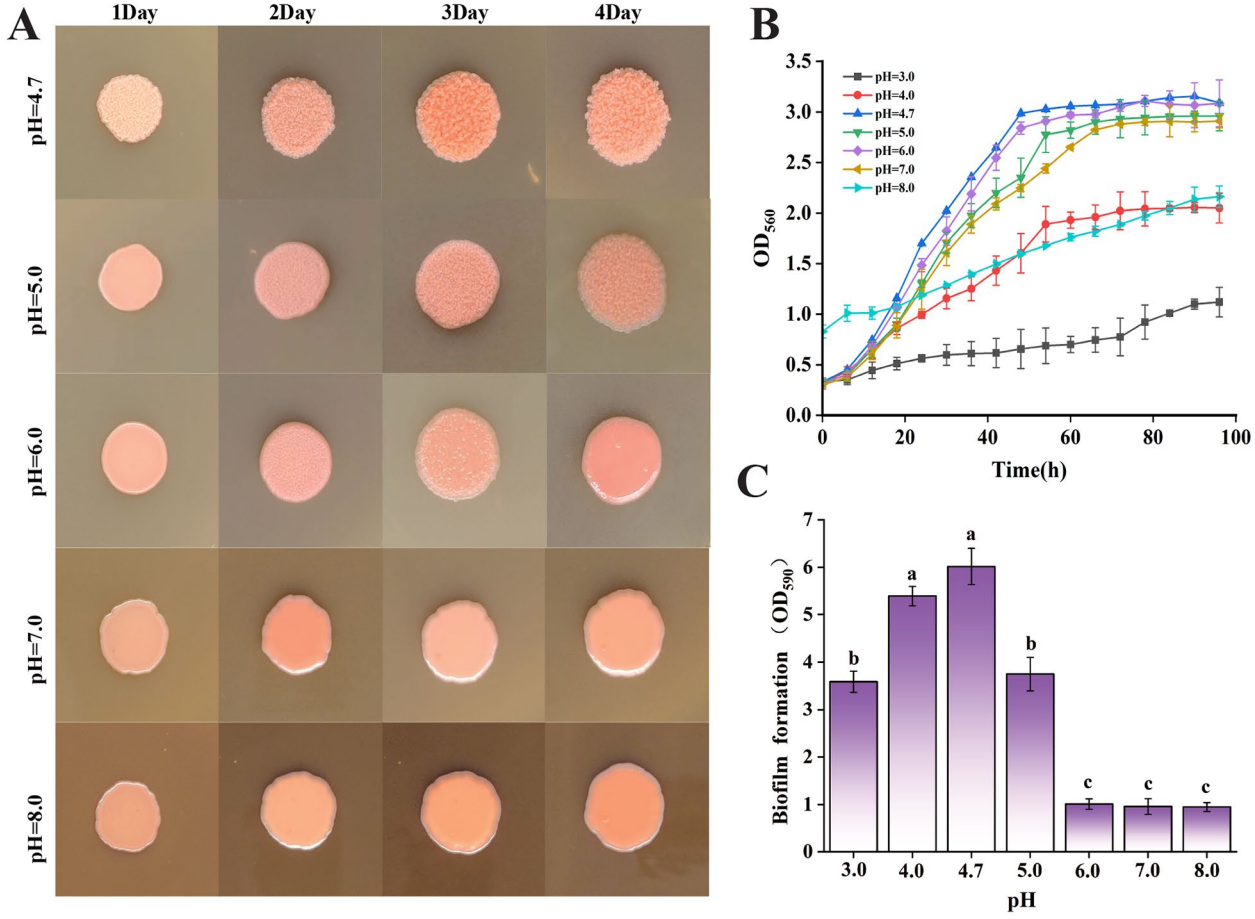

Fig. 1 Colony phenotype (**A**), growth curves (**B**) and biofilm production of *S. pararoseus* NGR under different pH conditions. All data are from three independent biological replicate means ± SE ($n = 3$). Different letters (a–c) indicate the degree of significance difference between treatments. Values with the same letter above the bar graph indicate no significant difference according to the Turkey test

significantly inhibited the growth of *S.pararoseus* NGR. The results depicted in Fig. 1-C demonstrate the biofilm synthesis capacity of *S. pararoseus* NGR under varying environmental conditions. It is evident that acidic conditions, specifically at pH 4.0 and 4.7, are the key factors that trigger enhanced biofilm synthesis in *S. pararoseus* NGR, with its biofilm production significantly surpassing that of other treatment groups.

Analysis of biofilm morphology and hydrophobicity of *S. pararoseus* NGR

The production of EPS in most biofilms happened between 48 and 72 h [33]. The electron microscopy results showed (Fig. 2) that at low magnification, the surfaces of the two colonies appeared distinctly different, with biofilm colonies (pH 4.7) having a very distinctive furrowed structure with undulating highs and lows on the surface (Fig. 2-E), whereas the surface of smooth colonies (pH 6.0) was flat (Fig. 2-A). Under high magnification to observe the internal cell arrangement, the biofilm colony (pH 4.7) had loose internal cell arrangement, large porosity, cell-to-cell adhesion by extracellular substances and fixed in a certain spatial position, with strong three-dimensionality (Fig. 2-F, G, H), while the smooth colony cell planar arrangement was more compact and two-dimensionality was stronger (Fig. 2-B, C, D).

In addition, hydrophobicity analyses showed that smooth colonies (pH 6.0) exhibited oil droplets in adherent cells with concomitant loss of turbidity compared to biofilm colony (pH 4.7) cells, and the lower aqueous phase demonstrated that non-biofilm colonies were more adherent to xylene compared to colony biofilm cells (Fig. 3-A, B).

Determination of biofilm polysaccharides, proteins and eDNA in *S. pararoseus* NGR

When *S. pararoseus* NGR was cultured on YPD solid medium, the abundances of polysaccharides, proteins, and eDNA in smooth colonies (pH 6.0) were 158.48, 49.65, and 0.08 mg/g, respectively. In contrast, the abundances of polysaccharides, proteins, and eDNA in

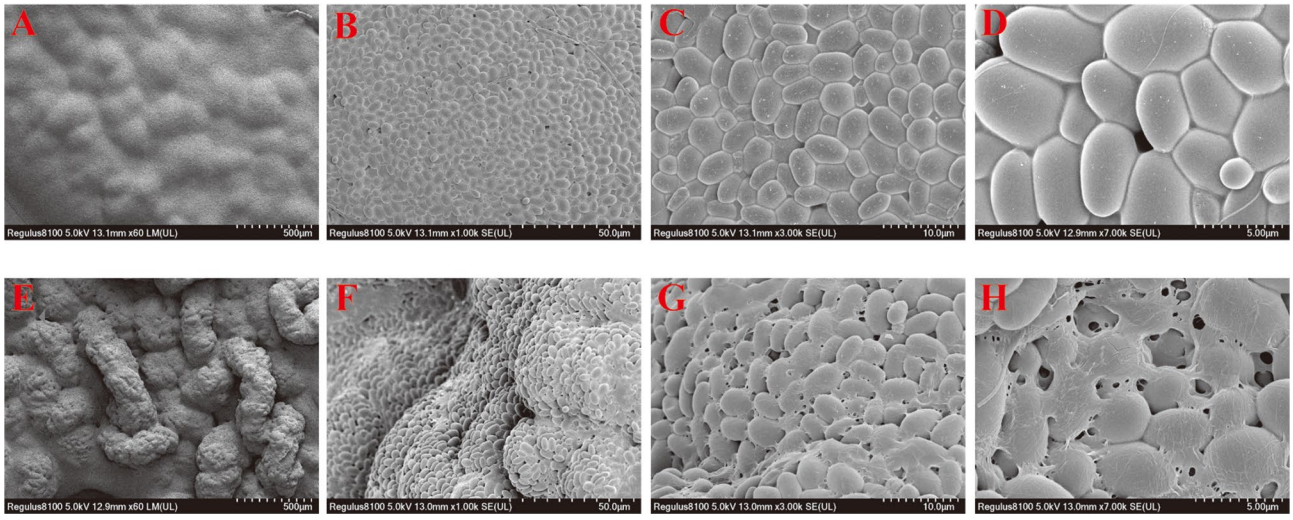

Fig. 2 Scanning electron microscopy observation of smooth colonies (pH 6.0) and wrinkled colonies (pH 4.7) in *S. pararoseus* NGR. **A-D** are smooth colonies. **E-H** are wrinkled colonies

wrinkled colonies (pH 4.7) were significantly higher at 285.50, 67.88, and 0.22 mg/g, respectively (Fig. 4A).

Similarly, when *S. pararoseus* NGR was cultured in YPD liquid medium, the abundances of polysaccharide, protein, and eDNA at pH 6.0 were 120.48, 28.01, and 0.09 mg/g, respectively. At pH 4.7, these values increased to 235.50, 58.84, and 0.21 mg/g, respectively (Fig. 4B).

Analysis of ROS, SOD, CAT, and T-AOC levels in biofilm and non-biofilm cells

It has been shown that biofilm cells improve the ability of strains to cope with environmental stresses [34]. To further the anti-oxidative stress capacity of both non-biofilm (pH 6.0) and biofilm (pH 4.7) cells in *S. pararoseus* NGR, the intracellular levels of ROS, SOD, CAT, and T-AOC were measured in two different colony morphologies. As shown in Fig. 5, the levels of ROS, SOD, CAT, and T-AOC were significantly higher in *S. pararoseus* NGR cells cultured either in solid or liquid at pH 4.7 than in non-biofilm (pH 6.0) cells, suggesting that biofilm formation has a stronger resistance to oxidative stress.

Effects of different pH culture conditions on carotenoid synthesis of *S. pararoseus* NGR

As shown in Fig. 6, the results show that the ability of *S. pararoseus* NGR to synthesize carotenoids at pH 4.7 is significantly higher than that at pH 6.0, regardless of whether *S. pararoseus* NGR is cultured in liquid or solid, indicating that the formation of biofilm helps to improve its pigment synthesis ability. The carotenoid yields of *S. pararoseus* NGR cultured in solid and liquid media at pH 4.7 for 96 h were 1370.3 and 1312.5 μg/g, respectively, which were significantly higher than those cultured at pH 6.0 (1203.8 and 1183.3 μg/g).

Transcriptome analysis

To identify DEGs of *S. pararoseus* NGR in biofilm cells (NGRA, pH 4.7) and non-biofilm cells (NGR, pH 6.0), we constructed six transcriptome libraries for transcriptome sequencing using Illumina Truseq SBS Kit (300cycles) sequencer. By sequencing the six cDNA libraries. DEGs were identified using a threshold of $|\log2FC| \geq 1$ or $FDR \leq 0.05$. As shown in Fig. 7A, B, a total of 56 genes were differentially expressed between biofilm (pH 4.7) and non-biofilm (pH 6.0) cells, of which 10 were up-regulated and 46 were down-regulated (Table S2). These DEGs may play key roles in response to acid stress and biofilm formation.

To further understand the biological role played by these DEGs and the biological processes involved, we performed GO and KEGG enrichment analysis, respectively. The top 15 items in the GO enrichment analysis were mainly related to cellular components (CC), biological processes (BP) and metabolic functions (MF). As shown in Fig. 7C, the top three categories significantly enriched in the CC category were intrinsic component of membrane (GO:0031224), integral component of membrane (GO:0016021) and cellular anatomical entity (GO:0110165). In the BP category, the top three significantly enriched categories were ion transmembrane transport (GO:0034220), transmembrane transport (GO:0055085), response to stress (GO:0006950). Among the MF categories, the top three significantly enriched categories were transmembrane transporter activity (GO:0022857), transporter activity (GO:0005215), and inorganic molecular entity transmembrane transporter activity (GO:0015318), respectively.

KEGG enrichment analysis showed that DEGs in biofilm cells (NGRA, pH 4.7) were enriched in a total of 20 pathways (Fig. 7-D). These include Tryptophan

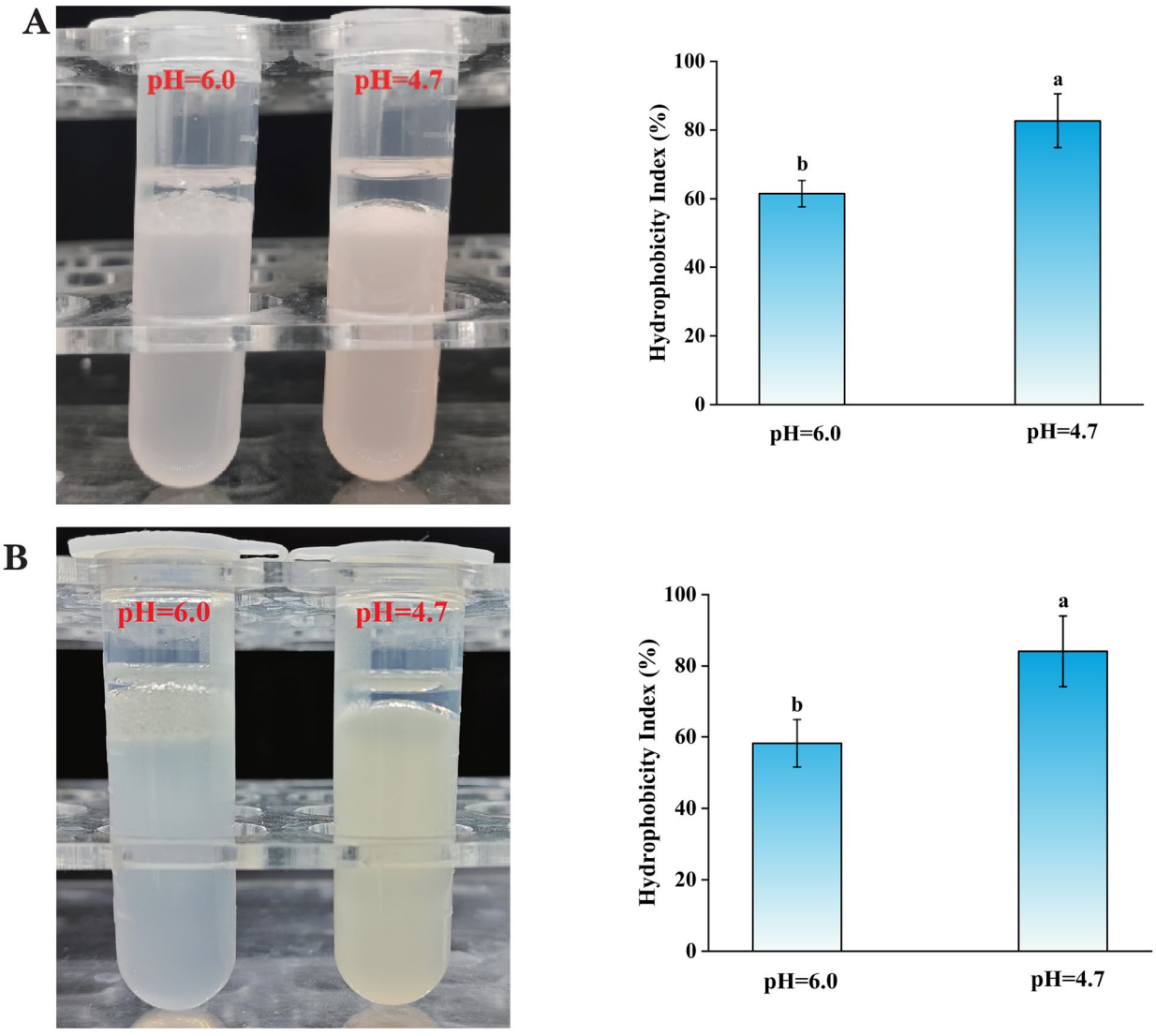

Fig. 3 The determination of hydrocarbon adhesion and cell hydrophobicity of *S. pararoseus* NGR cells in solid (**A**) and liquid (**A**) media under different pH conditions. All data are from three independent biological replicate means ± SE ($n = 3$). Different letters (a–b) indicate the degree of significant difference between treatments. Values with the same letter above the bar graph indicate no significant difference according to the Turkey test

metabolism (ko00380), Starch and sucrose metabolism (ko00500), Glutathione metabolism (ko00480), Glycine, serine and threonine metabolism (ko00260), Cysteine and methionine metabolism (ko00270), Biosynthesis of unsaturated fatty acids (ko00270), Biosynthesis of unsaturated fatty acids (ko01040), Fatty acid biosynthesis (ko00061), Glyoxylate and dicarboxylate metabolism (ko00630), Amino sugar and nucleotide sugar metabolism (ko00520), Nucleotide metabolism (ko01232), Pyrimidine metabolism (ko00240), Purine metabolism (ko00240), Pyrimidine metabolism (ko00230), and these pathways may be closely related to synthesis of biofilms in *S. pararoseus* NGR under acidic conditions.

Metabolomic analysis

Metabolomics profiles were analyzed using coupled LC-MS/MS. The results showed that a total of 759 metabolites were detected in both biofilm (pH 4.7) and non-biofilm (pH 6.0) cells in the positive ion mode, of which the number of metabolites annotated to KEGG database was 219, the number of metabolites annotated to HMDB database was 392, and the number of metabolites annotated to the LIPID MAPS database was 89 (Table S3). A total of 405 metabolites were detected in the negative ion mode, of which the number of metabolites annotated to the KEGG database was 143, the number of metabolites annotated to the HMDB database was 217, and the number of metabolites annotated to the LIPID MAPS database was 79. The differences in metabolites in biofilm (pH

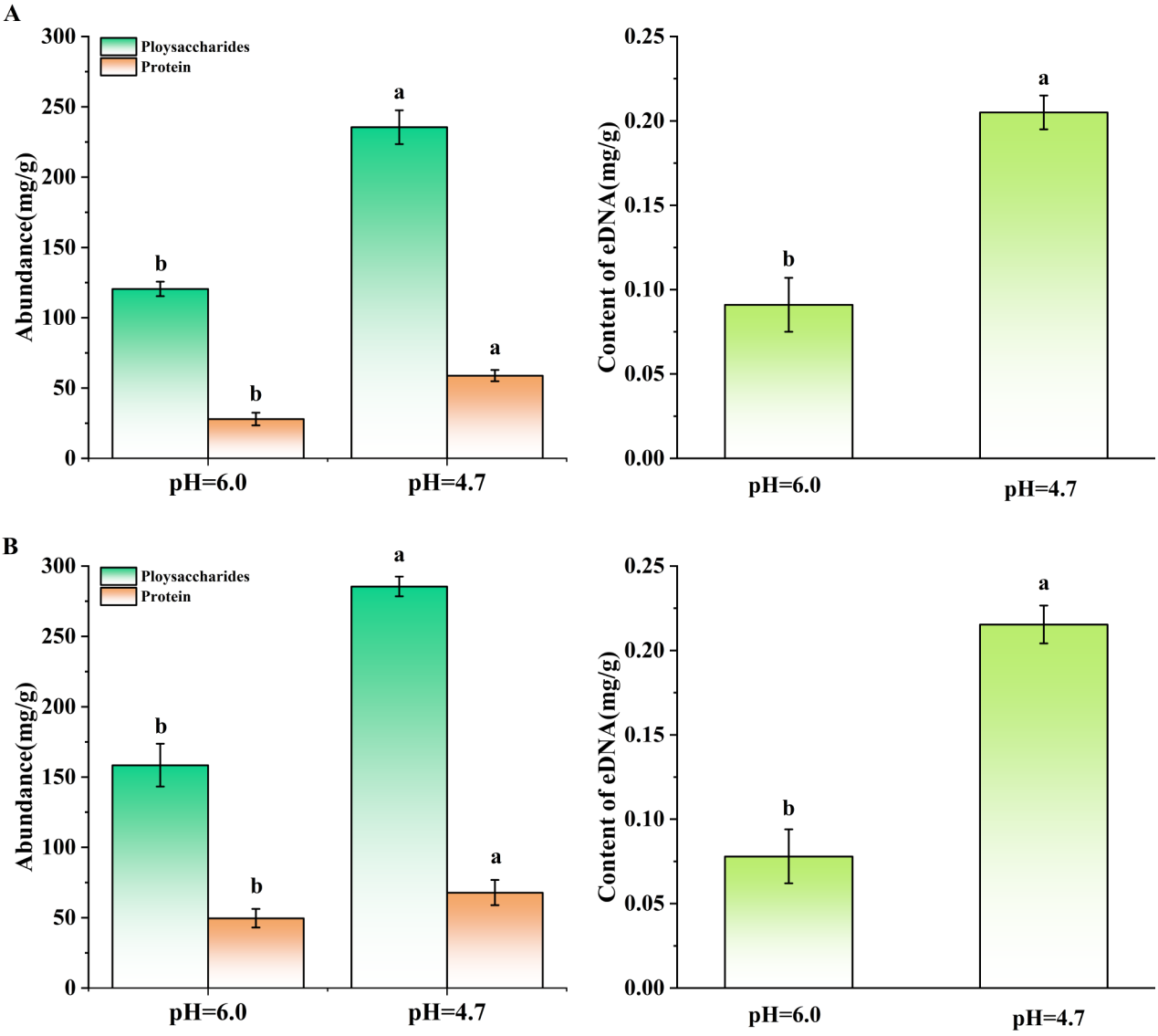

Fig. 4 Protein yield (mg/L), polysaccharide abundance (mg/L), and eDNA (mg/L) content in EPS synthesized by *S. pararoseus* NGR cells cultured in solid (**A**) and liquid media (**B**) at pH 6.0 and 4.7. All data are from three independent biological replicate means ± SE ($n = 3$). Different letters (a–b) indicate the degree of significant difference between treatments. Values with the same letter above the bar graph indicate no significant difference according to the Turkey test

4.7) and non-biofilm (pH 6.0) cells were then analyzed using the PLS-DA model and the OPLS-DA model. Both the PLS-DA model and the OPLS-DA model showed a good separation (biofilm cells vs. non-biofilm cells) for each sample pair ($p < 0.05$), and the alignment test showed that the method has a good model and has high reliability. Then, the VIP (Variable Importance in the Projection) value of the OPLS-DA model was used in combination with the pvalue of the independent samples t-test to find differentially expressed metabolites. Finally, a total of 341 differentially expressed metabolites were obtained in biofilm cells and non-biofilm cells, of which 135 were up-regulated metabolites and 206 were down-regulated metabolites (Fig. 8).

The accumulation of indole acetic acid, glutathione, mannose-6-phosphate, glucose-6-phosphate, NADH, stearic acid, inositol, and glycerol was significantly upregulated. Their synthesis is primarily associated with the tryptophan metabolism pathway and glutathione metabolism pathway within amino acid metabolism, pyruvate metabolism, the citric acid cycle (TCA cycle), and glyoxylate and dicarboxylic acid metabolism within carbohydrate metabolism. Additionally, it involves oxidative phosphorylation in energy metabolism, arachidonic acid metabolism, and fatty acid degradation, biosynthesis, and metabolism within lipid metabolism. The results are presented in Table S4.

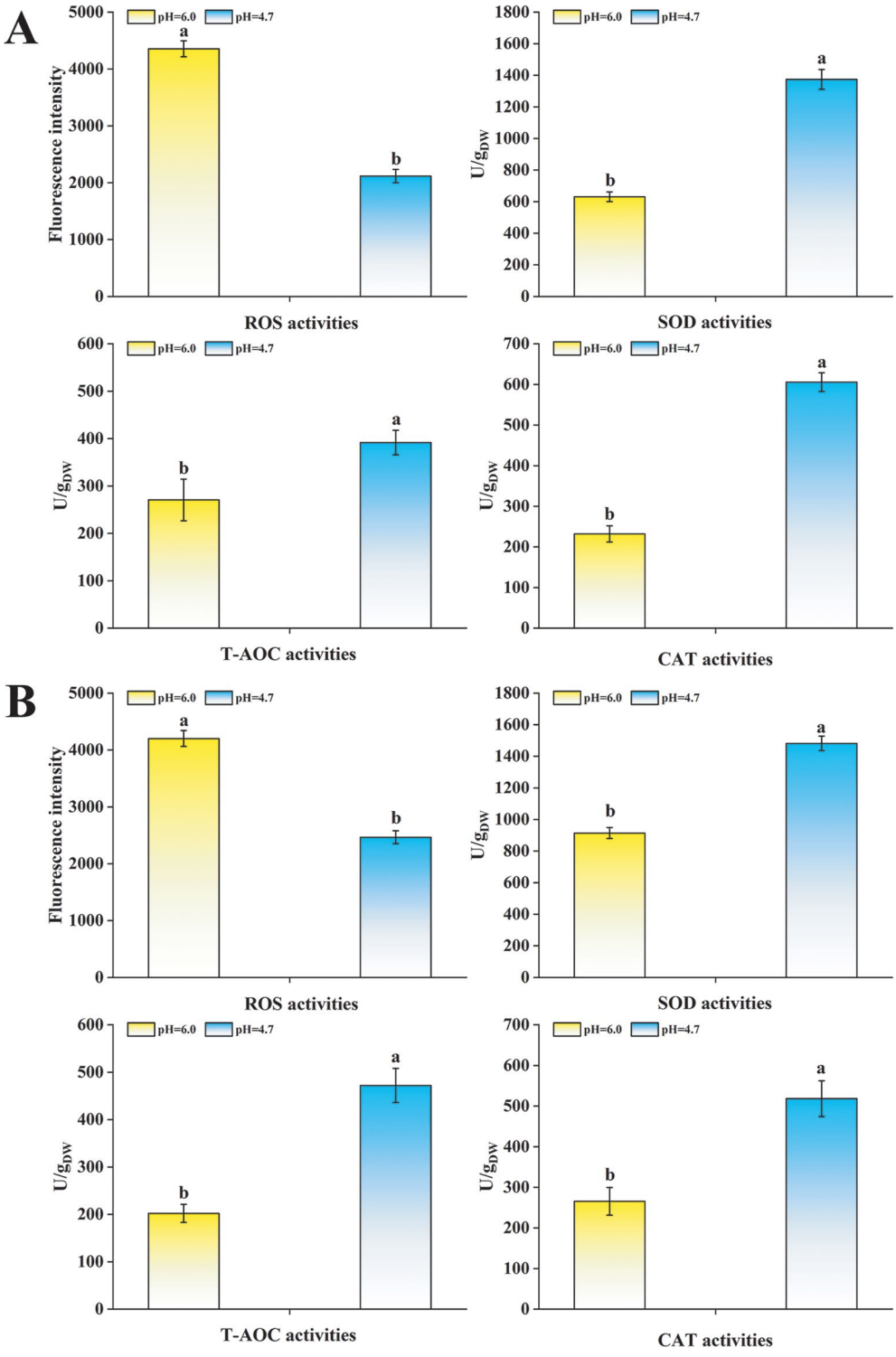

Fig. 5 Determination of intracellular ROS, SOD, T-AOC, and CAT levels in *S. pararoseus* NGR cells in solid (**A**) and liquid media (**B**) at pH 6.0 and 4.7. All data are from three independent biological replicate means ± SE ($n = 3$). All data represent means ± SE from three independent biological replicates ($n = 3$). Different letters (a–b) indicate the degree of significant difference between treatments. Values with the same letter above the bar graph indicate no significant difference according to the Tukey test

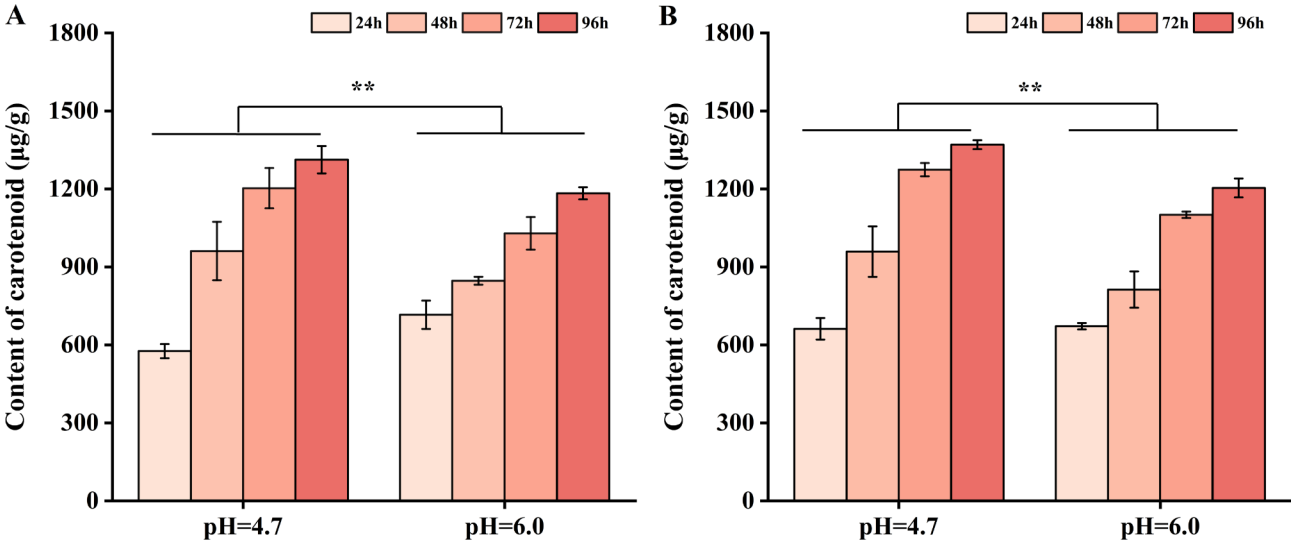

Fig. 6 Determination of carotenoid content in *S. pararoseus* NGR cells cultured in solid (**A**) and liquid media (**B**) at pH 6.0 and 4.7. All data are from three independent biological replicate means ± SE ($n = 3$). Statistical analyses were conducted using one-way ANOVA with GLMM, followed by Holm-Sidak's multiple-comparison tests (*, $P < 0.05$; **, $P < 0.01$)

To learn more differences in physiological defense information such as stress resistance between biofilm cells (pH 4.7) and non-biofilm cells (pH 6.0), the transcriptome and metabolome of biofilm cells and non-biofilm cells were analyzed jointly. Finally, 12 key metabolic pathways were obtained, which were mainly related to amino acid metabolism, carbohydrate metabolism, lipid metabolism and energy metabolism, mainly including Tryptophan metabolism, Starch and sucrose metabolism, Glutathione metabolism, Glycine, serine and threonine metabolism, Cysteine and methionine metabolism, Biosynthesis of unsaturated fatty acids, Fatty acid biosynthesis, Glyoxylate and dicarboxylate metabolism, Amino sugar and nucleotide sugar metabolism, Nucleotide metabolism, Purine metabolism and Pyrimidine metabolism, oxidative phosphorylation. The synthesis of *S. pararoseus* NGR into biofilm requires substrates and energy, and among these metabolic pathways, carbohydrate metabolic pathway, lipid metabolism and energy metabolic pathway can provide a large amount of energy and substrates for its own growth on the one hand, and help the cell to synthesize biofilm under acidic condition on the other hand. Amino acid metabolic pathway helps cells to provide precursors on the one hand, and synthesize antioxidant substances such as glutathione on the other hand to help cells resist ROS generated by environmental stresses. These metabolic pathways work together to make *S. pararoseus* NGR grow and reproduce by forming biofilm under acidic conditions.

Analysis of qPCR results

In order to verify the reliability of the RNA-seq data, we performed q-PCR to validate the relevant candidate genes in the transcriptome. 26Sr DNA was selected as the internal reference gene. As shown in Additional file 1: Table S5, the qPCR results of all genes were basically consistent with the RNA-seq data, indicating that the RNA-seq data were reliable in this study.

Discussion

The macrostructure of fungal colonies is highly dependent on environmental conditions [35]. Fungi are constantly challenged by environmental changes and produce wrinkled colonies containing large amounts of polysaccharides [36, 37], which are used as a marker to identify biofilm-forming strains to study the environmental conditions under which biofilm formation occurs [38]. Many environmental factors such as pH, temperature, nutrient conditions, ethanol, etc. stimulate microorganisms to produce biofilms, which help them to resist environmental stresses and increase their competitiveness and chances of survival in the environment [39]. Microorganisms with a biofilm lifestyle exhibit strong resistance and are accompanied by the production of large amounts of extracellular matrix and secondary metabolites. In this study, the effect of acidic conditions on the growth of *S. pararoseus* NGR was investigated, and the results showed that *S. pararoseus* NGR colony wrinkled and produced biofilm under acidic environment, and its growth was not only not inhibited under the condition of pH 4.7, but also the antioxidant capacity was stronger. This may be closely related to the fact that *S. pararoseus* NGR can resist acidic environmental stress to maintain normal cell growth, and it can help synthesize more metabolites by producing biofilm to resist environmental stress and improve its application in industrial

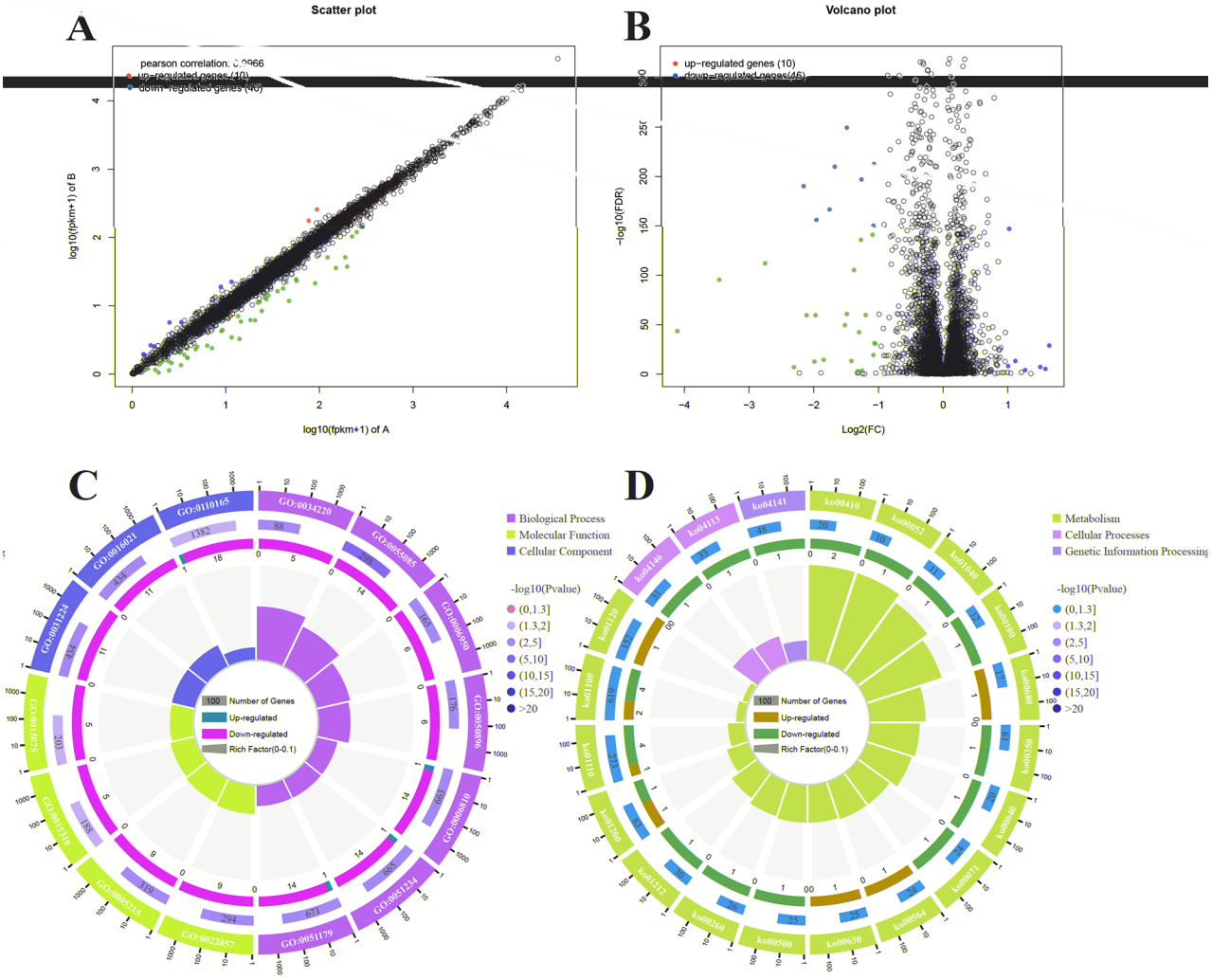

Fig. 7 Transcriptome analysis of NGRA (wrinkled colonies (pH 4.7)) and NGR (smooth colonies (pH 6.0)) in *S. pararoseus* NGR. (**A**) Scatter-plot of DEGs of NGRA and NGR. (**B**) Volcano plot of DEGs of NGRA and NGR. (**C**) Circos plots depicting GO enrichment analysis of DEGs. (**D**) Circos plots illustrating KEGG enrichment analysis of DEGs. Starting from the outer circle and moving inward the representation includes the top 20 enriched GO terms or KEGG pathways (ring 1), the number of background genes in the genome (ring 2), the number of up-regulated and down-regulated genes (ring 3), and the rich factor of DECs in corresponding GO terms or KEGG pathways (ring 4) are represented

fermentation. In addition, it provides a research basis for studying the extrinsic factors of macro-morphological changes in fungal colonies, and also provides a reference for studying other environmental factors affecting fungal morphology.

Studies have shown that pH is an important driver in determining biofilm formation, and biofilm production can in turn help to enhance microbial resistance [40, 41]. *Bacillus subtilis* and *Escherichia coli* showed higher biofilm production in the pH range of 5–6 [42], and this difference in the pH of the culture environment had a significant effect on the growth of the number of colonies on the biofilm. The growth rate of *Serriatia marcescens* biofilm at pH 9.0 is greater than that at pH 5.0 and 7.0 [43]. The biofilm of *Streptococcus mutans*, the causative agent of human caries, is influenced by pH, primarily through the production of lactic acid, which lowers the environmental pH. This acidification promotes biofilm formation and adherence to the tooth surface, enhances biofilm cell production, accelerates cell metabolism, and contributes to tooth erosion [44].

In this study, it was shown that the acidic environment of pH 4.7 was the key factor triggering biofilm production by *S. pararoseus* NGR. When *S. pararoseus* NGR was cultured at pH 4.7, its colony morphology was wrinkled, the cells were wrapped by a large amount of extracellular matrix, the internal arrangement of the cells was loose, the porosity was large, the cells were adhered and fixed to a certain spatial position by extracellular substances, and there was a strong three-dimensional structure, and the abundance of polysaccharides, proteins and eDNA in the extracellular EPS was significantly higher

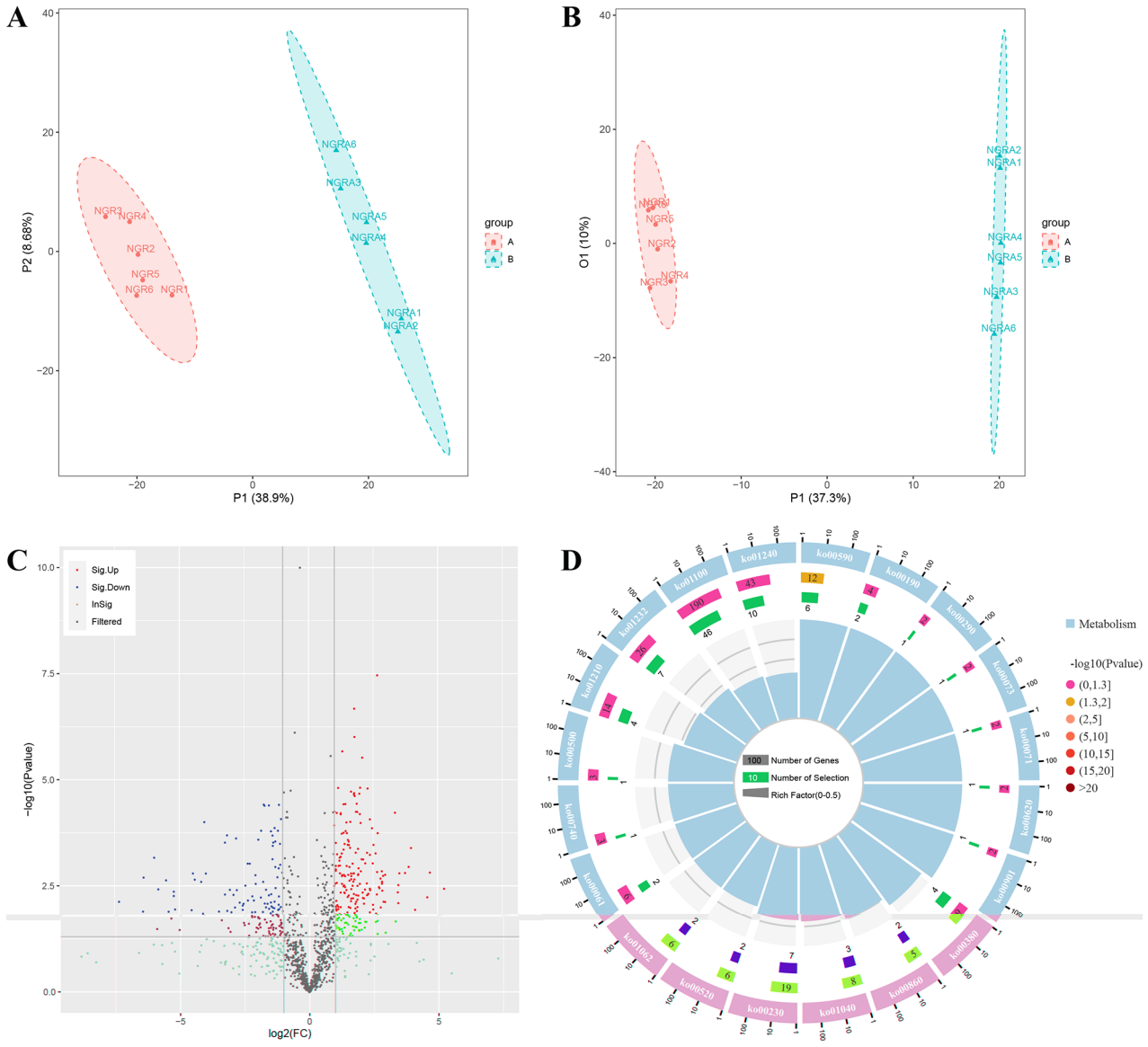

Fig. 8 Metabolome analysis of NGRA (wrinkled colonies (pH 4.7)) and NGR (smooth colonies (pH 6.0)) in *S. pararoseus* NGR. (**A**) PLS-DA plots comparing the treated group (NGRA) with the control group (NGR). (**B**) OPLS-DA plots comparing the treated group (NGRA) with the control group (NGR). (**C**) Volcanic plot of differential metabolites. (**D**) Circos plots of KEGG enrichment analysis of differential metabolites. From the outer circle to the inner, the top 20 enriched KEGG pathways (ring 1), numbers of background genes in the genome (ring 2), numbers of up-regulated and down-regulated genes (ring 3), and rich factor of differential metabolites in corresponding KEGG pathways (ring 4) are represented, respectively

than that in the other treatment groups. The most prominent characteristic of biofilm is the formation of a three-dimensional structure, which is closely linked to the production of extracellular EPS. EPS primarily consists of polysaccharides, eDNA, proteins, and lipids secreted by cells within the biofilm. These components are interconnected, polymerizing the cells and giving the colony a unique structural appearance. This enhances the stability of the biofilm and further aids cells in resisting stress and adapting to environmental conditions [45]. The results of transcriptome and metabolome analysis of cells under two different forms of wrinkled colonies (pH 4.7) and smooth colonies (pH 6.0) showed that carbohydrate metabolic pathways, amino acid metabolic pathways, lipid metabolic pathways and nucleic acid metabolic pathways were significantly enriched in wrinkled colony cells, and metabolic pathways were also changed. These changes were mainly caused by the acidic environment. Under normal conditions, ROS is naturally produced in the process of mitochondrial aerobic metabolism and maintains a dynamic balance [46]. In the face of environmental stress, ROS homeostasis is destroyed, and cells need to activate multiple pathways to help cells remove ROS in the body [47]. The anti-oxidative stress ability of the

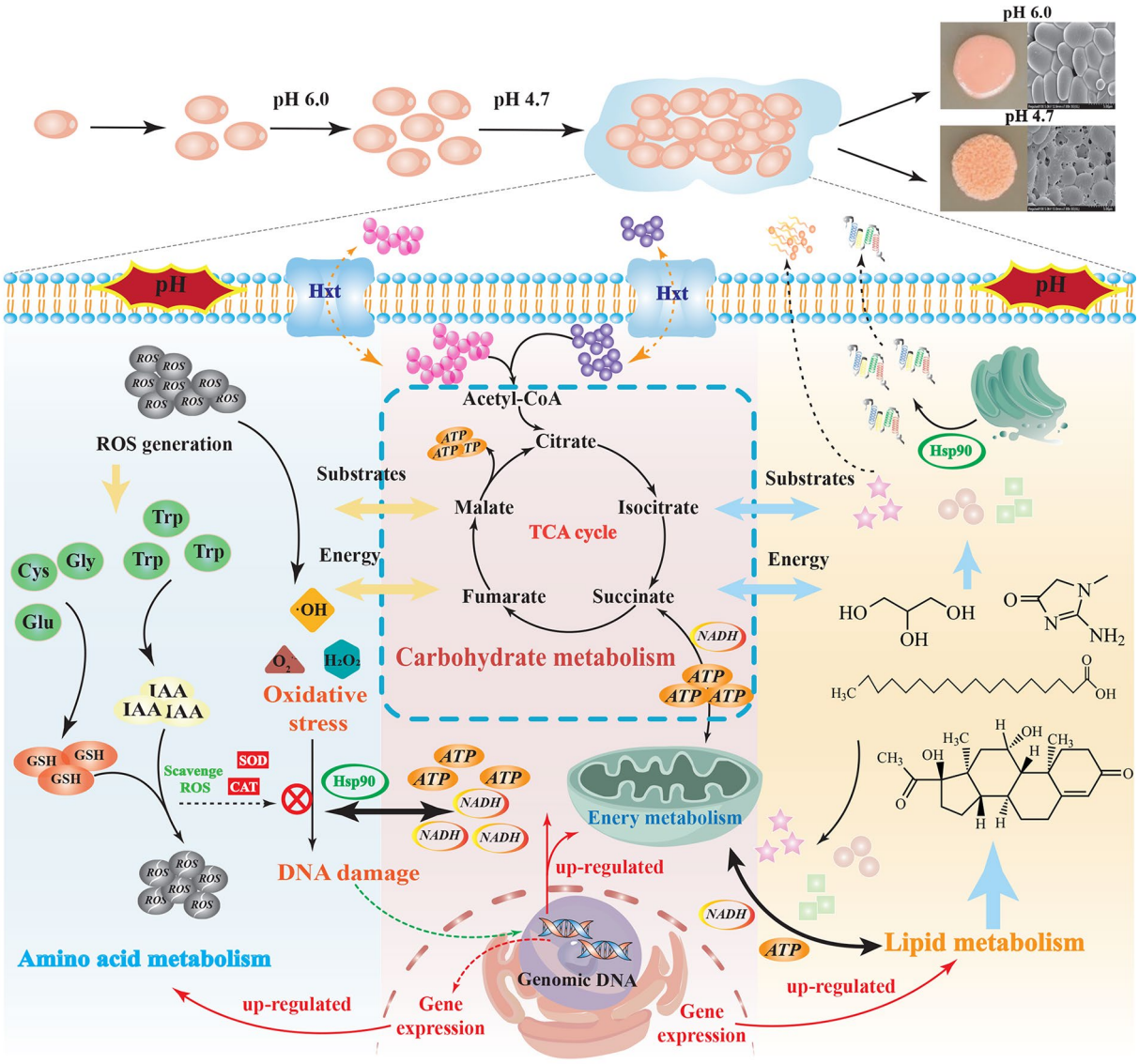

Fig. 9 Diagram of the mechanism of wrinkled biofilm colony formation in *S.pararoseus* NGR

two cells under the wrinkled colony (pH 4.7) and smooth colony (pH 6.0) of *S. pararoseus* NGR was tested. The results showed that the ROS level in the biofilm cells (pH 4.7) was significantly decreased, and the levels of SOD, T-AOC and CAT were also significantly higher than those in the non-biofilm cells (pH 6.0), indicating that the biofilm cells had stronger resistance than the non-biofilm cells.

In addition, carbohydrate metabolism, amino acid metabolism, and lipid metabolism play important roles in helping microorganisms resist adversity [48, 49]. Carbohydrate metabolism may be closely related to colony morphology changes and biofilm formation in *S. pararoseus* NGR, which forms wrinkled colonies in acidic environments, with cells wrapped and adhered together by a large number of EPS (e.g., Fig. 2-F, G, H), and a wide range of organic substances in the EPS, with carbohydrates and proteins as the main components, and a small amount of lipids and nucleic acids present [49, 50]. The polysaccharides in the biofilm EPS of *Candida albicans* are β-1,3-glucans, which enhance its drug resistance [51]; in the biofilm of dental plaque, the most abundant carbohydrate is glucan, which is produced extracellularly by sucrose-based transferase [52]. The main components of biofilm EPS of *Aspergillus fumigatus* are galactomannan, α-1,3-glucan and glucose [51]. In this study, a large number of biofilms were synthesized in *S. pararoseus* NGR at pH 4.7, and the carbohydrate pathway was significantly enriched, with significant accumulation of saccharides such as fructose, glucose, and mannose 6-phosphate, glucose 6-phosphate, and the expression of their related genes was significantly up-regulated. These carbohydrates may

serve as important components of EPS in the biofilm of *S. pararoseus* NGR, helping it to construct wrinkled colonies and form biofilms. In addition, we found that the expression of both *Hsp90* and *Hxt* genes were up-regulated. And *Hxt* gene can be used as the coding gene of hexose transporter carrier during the formation of biofilm in *Saccharomyces cerevisiae* to help the transport of sugars [53, 54]. Hsp90 is a heat shock protein, which has an important role in helping cells to resist adversity stress and form biofilm [55, 56]. Therefore, when *S. pararoseus* NGR is stimulated in an acidic environment, a large amount of carbohydrates are secreted out of the cell, and a portion of the carbohydrates (fructose, glucose, glucose 6-phosphate) are transported out of the cell to provide constituent materials for the biofilm via the Hxt sugar transporter carrier, while the other portion is used to maintain its own growth [57]. Previous studies have shown that cells in biofilms are in a high-density lifestyle [58, 59], and the wrinkled structure of the colonies may allow the cells to increase their access to oxygen in dense populations [37, 60]. Scanning electron microscopy of biofilm colonies of *S. pararoseus* NGR showed (Fig. 2-F) a certain porosity in their internal structure, which may be related to increasing the oxygen content inside the colony to meet the respiratory metabolism of the cells in biofilm mode. The results of the combined analysis indicated the accumulation of respiratory metabolites such as CO_2 and NADH associated with cellular respiratory metabolism, which could provide respiratory substrates to accelerate cellular metabolism in the high-density lifestyle [61].

Free amino acids also play an important role in cellular resistance to environmental stresses as key factors in the regulation of ROS homeostasis [62]. Notably, the results of the combined analysis showed that among the amino acid metabolic pathways, glutathione metabolism, IAA metabolic pathway were significantly enriched, and cysteine, glutamate, glycine, tryptophan were enriched and genetically significantly up-regulated. Among them, cysteine, glutamate and glycine are used as precursors for GSH synthesis, while tryptophan is a precursor substance for IAA synthesis [63, 64]. Studies have shown that GSH (γ -L-glutamyl-L-cysteinyl-glycine) play an important role in helping cells to scavenge ROS and resisting adversity [48, 65], whereas IAA also plays an important role in defending against adversity, as it reduces cellular oxidative stress, restores and increases free proline, ascorbic acid, and lipids and phenolic compounds in sums and stimulates cell growth in response to adversity [66, 67]. Therefore, the significant accumulation of cysteine, glutamate, glycine and tryptophan in the cells of wrinkled colonies synthesizes large amounts of glutathione and IAA to help the cells scavenge excess ROS to improve antioxidant properties and to help the cells resist acidic stress. In addition, lipids also play an important role in helping cellular resistance, and environmental stress induces the conversion of intracellular carbohydrate storage resources into lipids to burst excess ROS and indirectly improve the antioxidant capacity of cells [68, 69]. Lipid metabolisms are significantly enriched in metabolites such as stearic acid [70], inositol [71] and glycerol [72], and the related genes are significantly up-regulated, these increased carbohydrate, amino acid and lipid metabolites and their encoding genes may be important for *S. pararoseus* NGR in the formation of biofilms in cells under acid stress to resist environmental stress.

In summary, the fungal colony structure is affected by many factors of internal and external factors. Our results show that when *S. pararoseus* NGR is subjected to acidic environmental pressure, it will form a wrinkled colony and transform into a biofilm lifestyle (Fig. 9). At the same time, carbohydrate metabolism, amino acid metabolism, lipid metabolism, and nucleic acid metabolism in cells are up-regulated. The synthesis of a large amount of extracellular matrix provides precursors for the formation of biofilm and participates in the formation of biofilm. In addition, another function of carbohydrates is to act as energy substances, providing energy substances for cells in biofilm mode, improving cell metabolism, producing a large amount of CO_2, and maintaining the dynamic balance of intracellular ROS levels. Tryptophan, glycine, glutamic acid and cysteine are significantly accumulated in amino acid metabolism, and IAA and GSH are synthesized to help cells quench excessive ROS produced under acidic environmental conditions to maintain normal levels. Furthermore, the enriched lipids can also be used as substrates and energy for amino acid and carbohydrate metabolic pathways. Finally, the formation of biofilm in *S. pararoseus* NGR is realized by external environmental stimuli and internal perception and regulation to cope with changes in the surrounding environment, and ultimately help cells improve the level of carotenoid synthesis. These findings provide valuable insights into the regulation mechanisms of biofilm synthesis in *S. pararoseus* NGR and provide a theoretical foundation for future metabolic engineering strategies aimed at enhancing the industrial production and application of its metabolites.

Conclusion

In conclusion, it is shown that an acidic environment triggers wrinkling in colonies of *S. pararoseus* NGR and is accompanied by biofilm production. Wrinkled colonies exhibit a greater abundance of extracellular matrix and enhanced resistance to oxidative stress compared to smooth colonies, ultimately leading to improved carotenoid synthesis capability in the cells. Analysis of the transcriptome and metabolome results of cells in both colony morphologies showed that carbohydrate metabolism, amino acid metabolism, lipid metabolism, and nucleic acid metabolism were enriched in

metabolites and up-regulated in the cells of pleated colonies (pH 4.7) compared to those of smooth colonies (pH 6.0), and that carbohydrates, amino acids, lipids, and nucleic acids play an important role in the formation of biofilms in the *S. pararoseus* NGR and in resistance to acidic stress. This study reveals the response mechanism of *S. pararoseus* NGR to change the colony morphology against external environmental stresses, and also provides a basis for in-depth research on how cells contact signals to construct fixed colony structures and nutrient utilization during the various processes of biofilm formation, development, and dispersion in *S. pararoseus* NGR, enriching the research related to the changes in fungal biofilm and colony morphology. In addition, *S. pararoseus* NGR, as an important producer of carotenoids, is of great significance for the development and utilization of biofilm production to help it resist environmental changes and stabilize normal fermentation during industrial production.

Supplementary Information

The online version contains supplementary material available at https://doi.org/10.1186/s12934-024-02636-2.

Supplementary Material 1

Acknowledgements
We thank Shanghai Personal Biotechnology Co., Ltd. (Shanghai, China) for assisting in NGS and bioinformatic analysis.

Author contributions
DW-Conceptualization, Investigation, Writing – original draft, Writing – review & editing. NZ-Conceptualization, Writing – review & editing. CL-Investigation, Writing – review & editing. YW-Investigation. BC-Investigation. JL-Investigation. NZ-Supervision, Project administration, Funding acquisition. LB-Supervision, Funding acquisition, Project administration, Writing – review & editing.

Funding
This work was supported by the National Natural Science Foundation of China (31271818); International Cooperation Project of Universities in Liaoning Province (2023-01); Liaoning Province Rural Science and Technology Special Action Project (2022030673-JH5/104); Shenyang Science and Technology Project (22-319-2-13), and China Scholarship Council (CSC202208850002).

Data availability
No datasets were generated or analysed during the current study.

Declarations

Competing interests
The authors declare no competing interests.

Author details
[1]College of Land and Environment, Shenyang Agricultural University, Shenyang 110866, People's Republic of China
[2]College of Bioscience and Biotechnology, Shenyang Agricultural University, Shenyang 110866, People's Republic of China
[3]College of Agriculture and Biology, Zhongkai University of Agriculture and Engineering, Guangzhou 510225, People's Republic of China
[4]Innovative Institute for Plant Health, Zhongkai University of Agriculture and Engineering, Guangzhou 510225, People's Republic of China
[5]Key Laboratory of Green Prevention and Control on Fruits and Vegetables in South China, Ministry of Agriculture and Rural Affairs, Guangzhou 510225, People's Republic of China

Received: 27 March 2024 / Accepted: 24 December 2024
Published online: 07 January 2025

References

1. Li C, Li B, Zhang N, Wei N, Wang Q, Wang W, Xie Y, Zou H. Salt stress increases carotenoid production of *Sporidiobolus Pararoseus* NGR via torulene biosynthetic pathway. J Gen Appl Microbiol. 2019;65(3):111–20.
2. Li C, Zhang N, Li B, Xu Q, Song J, Wei N, Wang W, Zou H. Increased torulene accumulation in red yeast *Sporidiobolus Pararoseus* NGR as stress response to high salt conditions. Food Chem. 2017;237:1041–7.
3. Dworecka-Kaszak B, Kizerwetter-Świda M. Pseudomycelium forming *Rhodotorula* – unusual picture of biofilm. 2011;18(2):74–78.
4. Zara G, Farbo MG, Multineddu C, Migheli Q, Budroni M, Zara S, Mannazzu I. Exploring the Biodiversity of Red Yeasts for in Vitro and in vivo phenotypes relevant to Agri-Food-related processes. Fermentation. 2021;7(1):2.
5. Molla G, Motteran L, Piubelli L, Pilone MS, Pollegioni L. Regulation of D-amino acid oxidase expression in the yeast *Rhodotorula gracilis*. Yeast. 2003;20(12):1061–9.
6. Johnson EA. Biotechnology of non-*Saccharomyces* yeasts—the basidiomycetes. Appl Microbiol Biotechnol. 2013;97(17):7563–77.
7. Giannattasio S, Guaragnella N, Ždralević M, Marra E. Molecular mechanisms of *Saccharomyces cerevisiae* stress adaptation and programmed cell death in response to acetic acid. Front Microbiol, 2013;4.
8. Gasch AP. Comparative genomics of the environmental stress response in ascomycete fungi. Yeast. 2007;24(11):961–76.
9. Ramos S, García Acha I. A vegetative cycle of *Pullularia pullulans*. Trans Br Mycological Soc. 1975;64(1):129.
10. Wang F, Sethiya P, Hu X, Guo S, Chen Y, Li A, Tan K, Wong KH. Transcription in fungal conidia before dormancy produces phenotypically variable conidia that maximize survival in different environments. Nat Microbiol. 2021;6(8):1066–81.
11. Schultze LB, Maldonado A, Lussi A, Sculean A, Eick S. The impact of the pH value on Biofilm formation. Monogr Oral Sci. 2021;29:19.
12. Koshikawa T, Abe M, Nagi M, Miyazaki Y, Takemura H. Biofilm-formation capability depends on environmental oxygen concentrations in *Candida* species. J Infect Chemother. 2022;28(5):643–50.
13. Satyanarayana T, Kunze G. Yeast biofilms in the context of Human Health and Disease[M]//Singapore: Springer Singapore Pte. Limited, 2017:137–62.
14. Rodriguez DL, Quail MM, Hernday AD, Nobile CJ. Transcriptional circuits regulating developmental processes in *Candida albicans*. Front Cell Infect Microbiol, 2020;10.
15. Sauer K, Stoodley P, Goeres DM, Hall-Stoodley L, Burmølle M, Stewart PS, Bjarnsholt T. The biofilm life cycle: expanding the conceptual model of biofilm formation. Nat Rev Microbiol. 2022;20(10):608–20.
16. Branda SS, Vik Å, Friedman L, Kolter R. Biofilms: the matrix revisited. Trends Microbiol. 2005;13(1):20–6.
17. Kirisits MJ, Prost L, Starkey M, Parsek MR. Characterization of colony morphology variants isolated from *Pseudomonas aeruginosa* biofilms. Appl Environ Microbiol. 2005;71(8):4809–21.
18. Gupta R, Schuster M. Quorum sensing modulates colony morphology through alkyl quinolones in *Pseudomonas aeruginosa*. BMC Microbiol. 2012;12:30.
19. Yin W, Wang Y, Liu L, He J, Biofilms. The Microbial Protective Clothing in Extreme environments. Int J Mol Sci. 2019;20(14):3423.
20. Hurlow J, Couch K, Laforet K, Bolton L, Metcalf D, Bowler P. Clinical biofilms: a challenging Frontier in Wound Care. Adv Wound Care. 2015;4(5):295–301.
21. Gattlen J, Zinn M, Guimond S, Körner E, Amberg C, Mauclaire L. Biofilm formation by the yeast *Rhodotorula mucilaginosa*: process, repeatability and cell attachment in a continuous biofilm reactor. Biofouling (Chur Switzerland). 2011;27(9):979–91.
22. Donlan RM, Costerton JW, Biofilms. Survival mechanisms of clinically relevant Microorganisms. Journals ASM org. 2002;15(2):167–93.
23. Donlan RM. Biofilms: microbial life on surfaces. Emerg Infect Dis. 2002;8(9):881–90.
24. Enfert JB, A, C. *Candida albicans* biofilms: building a heterogeneous, drug-tolerant environment. Curr Opin Microbiol. 2013;16:1–16.
25. Kawarai T, Furukawa S, Ogihara H, Yamasaki M. Mixed-species biofilm formation by lactic acid Bacteria and Rice Wine yeasts. Appl Environ Microbiol. 2007;73(14):4673–6.

26. Cerca N, Pier GB, Vilanova M, Oliveira R, Azeredo J. Quantitative analysis of adhesion and biofilm formation on hydrophilic and hydrophobic surfaces of clinical isolates of *Staphylococcus epidermidis*. Res Microbiol. 2005;156(4):506–14.
27. Absolom DR. The role of bacterial hydrophobicity in infection: bacterial adhesion and phagocytic ingestion. Can J Microbiol. 1988;34(3):287–98.
28. Rosenberg M. Basic and applied aspects of microbial adhesion at the hydrocarbon:water interface. Crit Rev Microbiol. 1991;18(2):159.
29. Breitenbach R, Silbernagl D, Toepel J, Sturm H, Broughton WJ, Sassaki GL, Gorbushina AA. Corrosive extracellular polysaccharides of the rock-inhabiting model fungus *Knufia petricola*. Extremophiles. 2018;22(2):165–75.
30. Homero U, Tortella G, Sandoval E, Cuozzo SA. Extracellular polymeric substances (EPS) produced by *Streptomyces sp*. biofilms: Chemical composition and anticancer properties. Microbiol Res. 2021;253:126877.
31. Ke X, Xu J, Wang X, Zhu B, Han F, Tang L, Jiang Z, Gu T, Li Z. Extracting extracellular polymeric substances from fungi in contrasts: from quantity to quality. Appl Microbiol Biotechnol. 2023;107(2–3):943–54.
32. Kagi JHR, Schaffer A. Biochemistry of Metallothionein. Perspect Biochem, 1988;27(23).
33. Memariani H, Memariani M, Ghasemian A. An overview on anti-biofilm properties of quercetin against bacterial pathogens. World J Microbiol Biotechnol, 2019;35(9).
34. Plocek V, Váchová L, Šťovíček V, Palková Z. Cell distribution within yeast colonies and colony biofilms: how structure develops. Int J Mol Sci. 2020;21(11):3873.
35. Kowalski CH, Cramer RA. If looks could kill: fungal macroscopic morphology and virulence. PLoS Pathog. 2020;16(6):e1008612.
36. Khider M, Willassen NP, Hansen H. The alternative sigma factor RpoQ regulates colony morphology, biofilm formation and motility in the fish pathogen *Aliivibrio salmonicida*. BMC Microbiol, 2018;18(1).
37. Morales DK, Grahl N, Okegbe C, Dietrich LEP, Jacobs NJ, Hogan DA, Berman J. Control of *Candida albicans* metabolism and biofilm formation by *Pseudomonas aeruginosa* phenazines. mBio. 2013;4(1):e526.
38. Ray VA, Morris AR, Visick KL. A semi-quantitative approach to assess biofilm formation using wrinkled colony development. J Vis Exp, 2012;(64):e4035.
39. Granek JA, Magwene PM. Environmental and genetic determinants of colony morphology in yeast. PLoS Genet. 2010;6(1):e1000823.
40. Mathlouthi A, Pennacchietti E, De Biase D. Effect of temperature, pH and plasmids on in Vitro Biofilm formation in *Escherichia coli*. Acta Naturae. 2018;10(4):129–32.
41. Vaezi SS, Elahe P A T F. Biofilm Formation Of *Staphylococcus Aureus* In Presence Of Sodium Chloride, Ethanol And Ph Different Levels And Application Of Artificial Neural Networks To Describe The Combined Effect Of Them. Int J Med Invest, 2021;10(2):58–73.
42. Ganchev I. Biofilm formation *between Bacillus* Subtilis and Escherichia Coli K-12 strains at acidic and oxidative stress. Sci J Chem. 2019;7(1):15.
43. Harimawan A, Devianto H, Kurniawan IC, Utomo JC. Influence of initial Ph solution on biofilm formation and corrosion of carbon steel by *Serratia marcescens*. Reaktor (Semarang Indonesia). 2017;17(2):89–95.
44. Kawarai T, Narisawa N, Suzuki Y, Nagasawa R, Senpuku H. *Streptococcus mutans* biofilm formation is dependent on extracellular DNA in primary low pH conditions. J Oral Biosci. 2016;58(2):55–61.
45. Wang D, Zeng N, Li C, Li Z, Zhang N, Li B. Fungal biofilm formation and its regulatory mechanism. Heliyon. 2024;10(12):e32766.
46. Yang H, Lee T. Antioxidant enzymes as redox-based biomarkers: a brief review. BMB Rep. 2015;48(4):200–8.
47. Li C, Cheng P, Li Z, Xu Y, Sun Y, Qin D, Yu G. Transcriptomic and metabolomic analyses provide insights into the enhancement of Torulene and Torularhodin Production in *Rhodotorula glutinis* ZHK under Moderate Salt conditions. J Agric Food Chem. 2021;69(38):11523–33.
48. Liu Z, Zhou Z, Wang L, Li M, Wang W, Yi Q, Huang S, Song L. Dopamine and serotonin modulate free amino acids production and Na+/K+ pump activity in Chinese Mitten crab *Eriocheir sinensis* under Acute Salinity stress. Frontiers in Physiology, 2018;9.
49. Flemming H, Wingender J. The biofilm matrix. Nat Rev Microbiol. 2010;8(9):623–33.
50. Sutherland IW. Exopolysaccharides in biofilms, flocs and related structures. Water Sci Technol. 2001;43(6):77–86.
51. Reichhardt C, Stevens DA, Cegelski L. Fungal biofilm composition and opportunities in drug discovery. Future Med Chem. 2016;8(12):1455–68.
52. Jakubovics NS, Goodman SD, Mashburn Warren L, Stafford GP, Cieplik F. The dental plaque biofilm matrix. Periodontol 2000. 2021;86(1):32–56.
53. Pursell NW, Mishra P, Bolon DNA. Solubility-promoting function of Hsp90 contributes to client maturation and robust cell growth. Eukaryot Cell. 2012;11(8):1033–41.
54. Verstrepen KJ, Iserentant D, Malcorps P, Derdelinckx G, Van Dijck P, Winderickx J, Pretorius IS, Thevelein JM, Delvaux FR. Glucose and sucrose: hazardous fast-food for industrial yeast? Trends Biotechnol. 2004;22(10):531–7.
55. Shapiro RS, Uppuluri P, Zaas AK, Collins C, Senn H, Perfect JR, Heitman J, Cowen LE. Hsp90 orchestrates temperature-dependent *Candida albicans* morphogenesis via Ras1-PKA signaling. Curr Biol. 2009;19(8):621–9.
56. Robbins N, Uppuluri P, Nett J, Rajendran R, Ramage G, Lopez-Ribot JL, Andes D, Cowen LE, May RC. Hsp90 governs dispersion and drug resistance of fungal biofilms. PLoS Pathog. 2011;7(9):e1002257.
57. Park S, Dingemans J, Gowett M, Sauer K. Glucose-6-Phosphate acts as an Extracellular Signal of SagS to modulate *Pseudomonas aeruginosa* c-di-GMP levels, attachment, and Biofilm formation. mSphere, 2021;6(1).
58. Stephen M, Hunt E M W. B. Hypothesis for the role of nutrient starvation in Biofilm detachment. Appl Environ Microbiol. 2004;70(12):7418–25.
59. Sauer K, Cullen A H R MC. L. characterization of Nutrient-Induced Dispersion in *Pseudomonas aeruginosa* PAO1 Biofilm. J Bacteriol. 2004;186(21):7312–26.
60. Dietrich LEP, Okegbe C, Price-Whelan A, Sakhtah H, Hunter RC, Newman DK. Bacterial community morphogenesis is intimately linked to the Intracellular Redox State. J Bacteriol. 2013;195(7):1371–80.
61. Luengo A, Li Z, Gui DY, Sullivan LB, Zagorulya M, Do BT, Ferreira R, Naamati A, Ali A, Lewis CA, Thomas CJ, Spranger S, Matheson NJ, Vander HM. Increased demand for NAD(+) relative to ATP drives aerobic glycolysis. Mol Cell. 2021;81(4):691–707.
62. Ahmadi FI, Karimi K, Struik PC. Effect of exogenous application of methyl jasmonate on physiological and biochemical characteristics of Brassica napus L. Cv. Talaye under salinity stress. South Afr J Bot. 2018;115:5–11.
63. Ikram M, Ali N, Jan G, Jan FG, Rahman IU, Iqbal A, Hamayun M, Berta G. IAA producing fungal endophyte *Penicillium Roqueforti* Thom., enhances stress tolerance and nutrients uptake in wheat plants grown on heavy metal contaminated soils. PLoS ONE. 2018;13(11):e208150.
64. Golovatskaya IF, Kadyrbaev MK, Boyko EV. Protective role of Melatonin and IAA in the regulation of resistance of Potato regenerants to Cold stress. Potato Res. 2024;67(2):421–49.
65. Aboushousha R, van der Velden J, Hamilton N, Peng Z, MacPherson M, Erickson C, White S, Wouters EFM, Reynaert NL, Seward DJ, Li J, Janssen-Heininger. Y M W. Glutaredoxin attenuates glutathione levels via deglutathionylation of Otub1 and subsequent destabilization of system xC. Sci Adv. 2023;9(37):i5192.
66. Iglesias MJ, Terrile MC, Casalongué CA. Auxin and salicylic acid signalings counteract the regulation of adaptive responses to stress. Plant Signal Behav. 2011;6(3):452–4.
67. Golovatskaya IF, Kadyrbaev MK, Boyko EV. Protective role of Melatonin and IAA in the regulation of resistance of Potato regenerants to Cold stress. Potato Research; 2023.
68. Meijer HJG, van Himbergen JAJ, Musgrave A, Munnik T. Acclimation to salt modifies the activation of several osmotic stress-activated lipid signalling pathways in Chlamydomonas. Phytochemistry. 2017;135:64–72.
69. Wang T, Ge H, Liu T, Tian X, Wang Z, Guo M, Chu J, Zhuang Y. Salt stress induced lipid accumulation in heterotrophic culture cells of *Chlorella protothecoides*: mechanisms based on the multi-level analysis of oxidative response, key enzyme activity and biochemical alteration. J Biotechnol. 2016;228:18–27.
70. Tao Wang HGTL, Zhuang Y. Salt stress induced lipid accumulation in heterotrophic culture cells of *Chlorella protothecoides*: mechanisms based on the multi-level analysis of oxidative response, key enzyme activity and biochemical alteration. J Biotechnol. 2016;228:18–27.
71. Xiao X, Qiuli W, Xin M, Duoyong L, Zhenggang GA, Zhang X. Physiological Biochemistry-CombinedTranscriptomic analysis reveals mechanism of *Bacillus cereus* G2 improved salt stress tolerance of *Glycyrrhiza Uralensis* Fisch. Seedlings by balancing Carbohydrate Metabolism. Front Plant Sci. 2022;12:1–21.
72. Zeng N, Zhang N, Ma X, Wang Y, Zhang Y, Wang D, Pu F, Li B. Transcriptomics Integrated with metabolomics: assessing the Central Metabolism of different cells after cell differentiation in *Aureobasidium pullulans* NG. J fungi (Basel). 2022;8(8):882.

Publisher's note